

Supplementary Data

Supplementary Methods:

Release kinetics of VEGF from collagen sponges in vivo. 20µg of human recombinant VEGF165 was labeled with AlexaFluor 555 (Microscale Protein Labeling Kit; Invitrogen) as described in manufacturer's instructions. 0.5µg fluorescence labelled VEGF, loaded in collagen sponges, was inserted into the injury region when the cortical defect was generated. Tibial segments including the defect hole region were carefully isolated at various time points after surgery, and observed under confocal microscope. A z-series file up to 200µm deep from the surface was acquired in area covering the hole region. The maximum intensity projection from the z-series images was chosen for the analysis of fluorescence density using Image J. The fluorescence intensities of samples at different time points represent the relative amount of VEGF remaining in the sponge.

Isolation of murine articular chondrocytes. The primary joint chondrocytes were isolated from femoral head, femoral condyles and tibial plateau of 5-days old mice according to a protocol described previously (1). The primary chondrocytes were cultured in 10% DMEM with 10% FBS.

CCK-8 cell proliferation assay. 4,000 BMSCs were seeded in each well of 96-well plate. The next day, cells were given α MEM medium (10% or 2% FBS) containing vehicle, 10-40ng/ml recombinant VEGF (R&D) and/or 2-40ng/ml recombinant PDGF-BB (R&D). After two days of additional culture, 10µl cell counting kit 8 (CCK-8, Sigma-Aldrich) was added to each well and incubated for 3 hours. Absorbance at 450 nm, representing relative cell numbers, was measured using a microplate reader. For chondrocyte proliferation, 2000 primary chondrocytes were seeded in each well of 96-well plate. The next day, cells were given the complete culture medium with 10-40ng/ml recombinant VEGF (R&D). Cell numbers were monitored at day1, 3, 5, and 7 after seeding with medium change every other day.

Complete blood analysis. Mice were placed under general anesthesia, and peripheral blood was collected from the heart. About 20 µl of blood samples were analyzed by Hemavet 950 Chemistry Analyzer (Drew Scientific Inc.).

Supplementary Reference:

1. Gosset M, Berenbaum F, Thirion S, and Jacques C. Primary culture and phenotyping of murine chondrocytes. *Nat Protoc.* 2008;3(8):1253-60.

Supplementary Figures

Figure S1

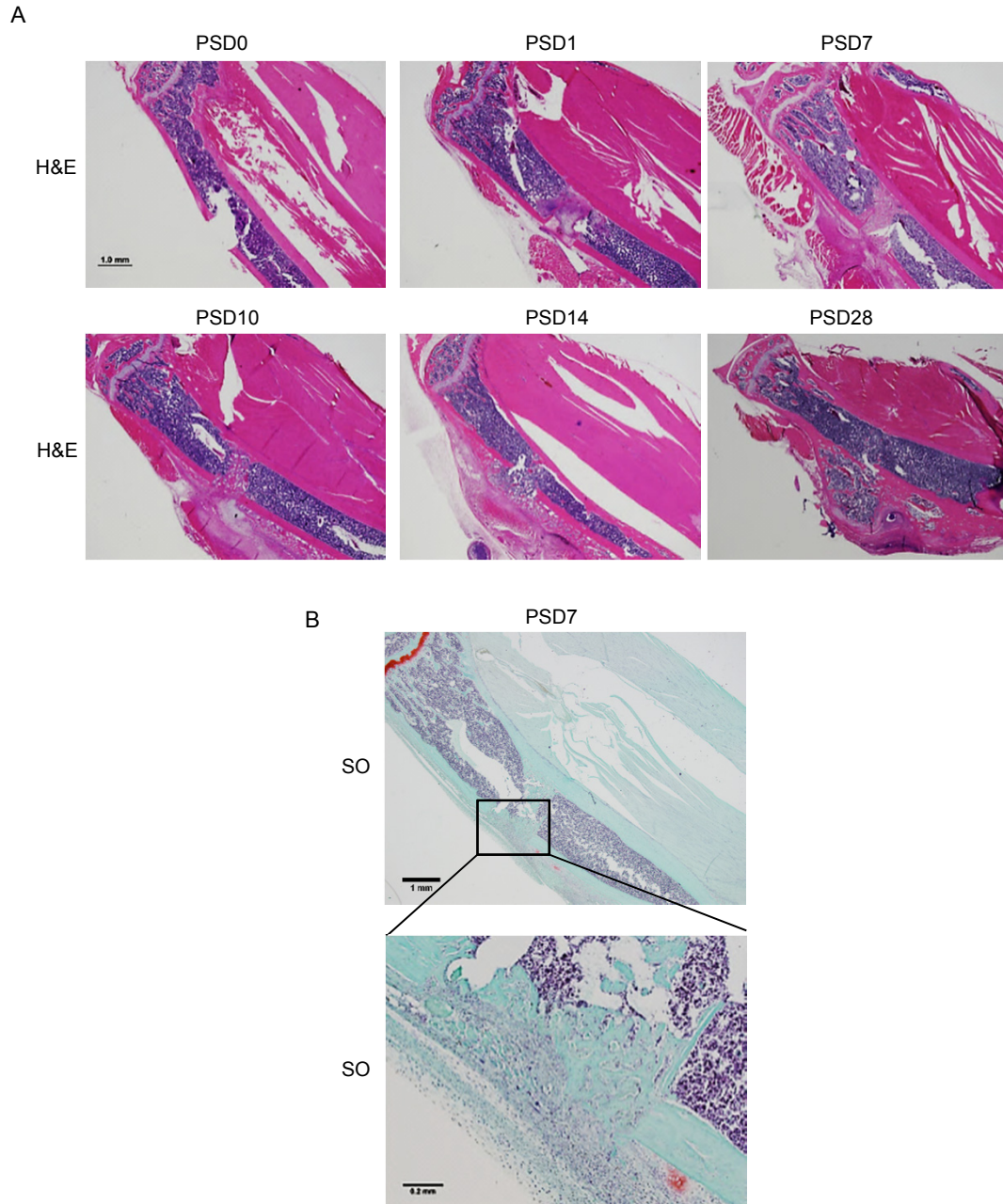


Figure S1. **Repair of cortical defects recapitulates most steps in fracture healing.** (A) Representative histological images of injury tibiae at various time points after surgery. Scale bar: 1mm. (B) Safranin O (SO)-stained sections from wild type mice shows absence of SO-positive cartilage in hole region and presence of cartilage in injured periosteum at PSD7. Scale bar: 1mm (upper image), 200µm (lower image). Representative image from 3 mice at each time point.

Figure S2

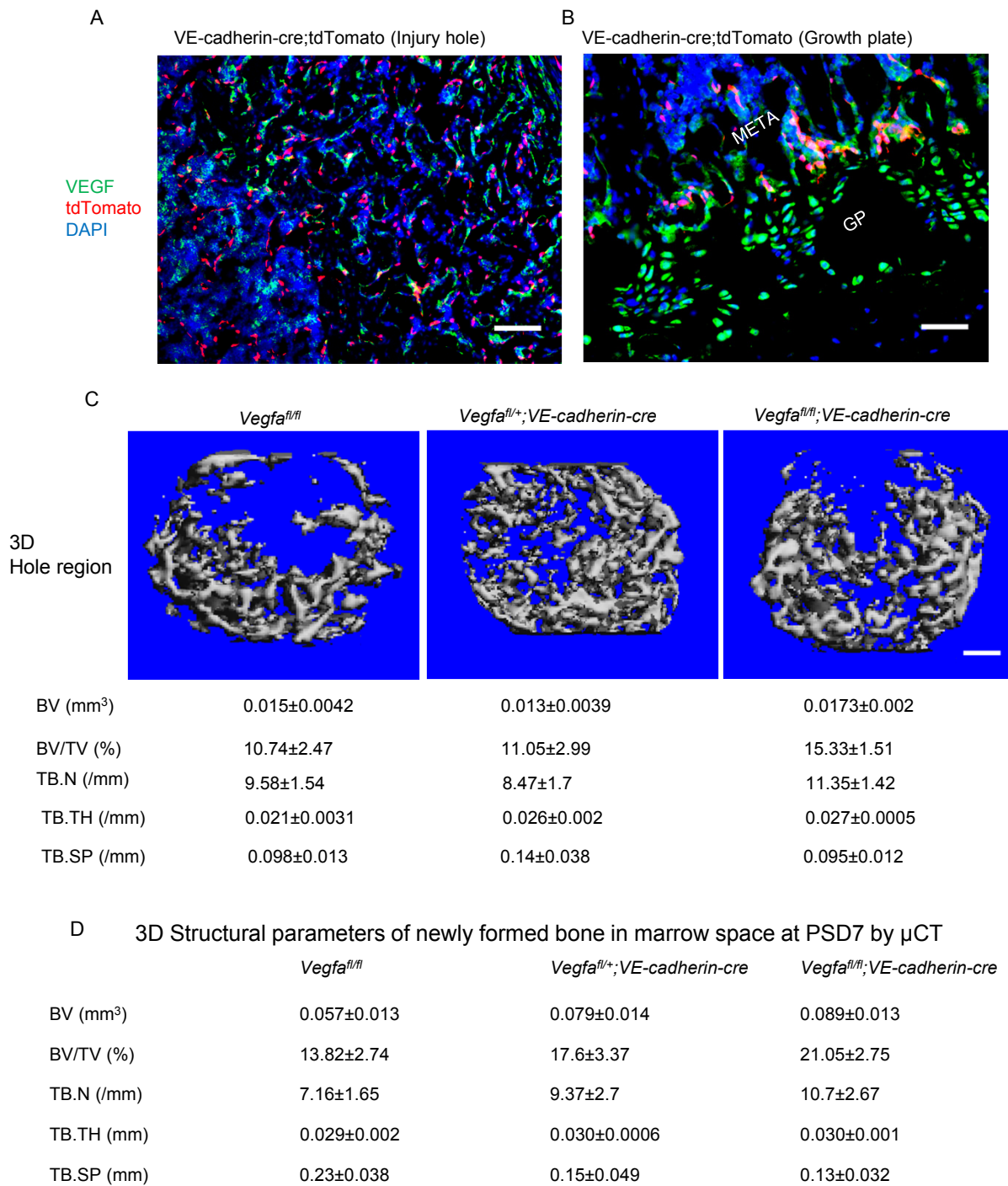


Figure S2. **Deletion of *Vegfa* in endothelial cells does not affect intramembranous bone formation during bone repair.** (A) Small amounts of anti-VEGF staining in tdTomato-positive endothelial cells in defects of *VE-cadherin;tdTomato* mice at PSD7. (B) Some tdTomato-positive endothelial cells in metaphyseal vessels express VEGF. GP: growth plate. META: metaphysis. (C) 3D-reconstruction of mineralized bone formed in hole region of mice at PSD7 and 3D structural parameters by μ CT analysis. (D) 3D μ CT-based structural parameters of mineralized bone formed in wounded bone marrow space of mice at PSD7. Representative image from 3 mice (A, B). N=5-6 for each genotype (C, D). Scale bars: 50 μ m (B), 100 μ m (A, C). ANOVA with Tukey's post-hoc test was used.

Figure S3

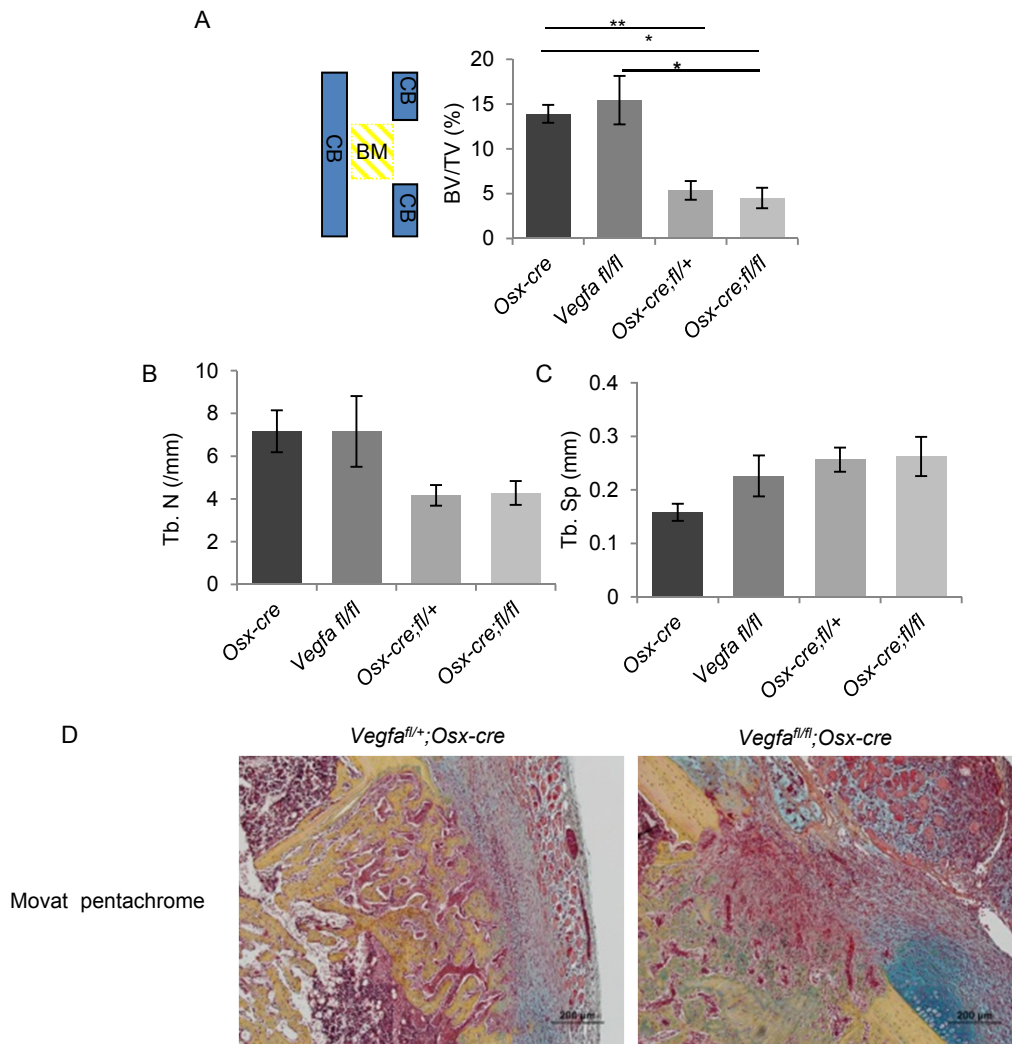


Figure S3. **Delayed intramembranous bone formation in defects of *Vegfa*^{fl/fl};*Osx-cre* mice at PSD7.** (A-C) 3D μ CT-based structural parameters of mineralized bone formed in wounded marrow (yellow area). CB: cortical bone, N=6. (D) Movat pentachrome staining shows histological details in hole region. Dense collagen fibers stained yellow and muscle and loose fibrous tissues stained red. Representative image from 3 mice for each genotype. Scale bar: 200 μ m. ANOVA with Tukey's post-hoc test was used *, $P<0.01$; **, $P<0.05$.

Figure S5

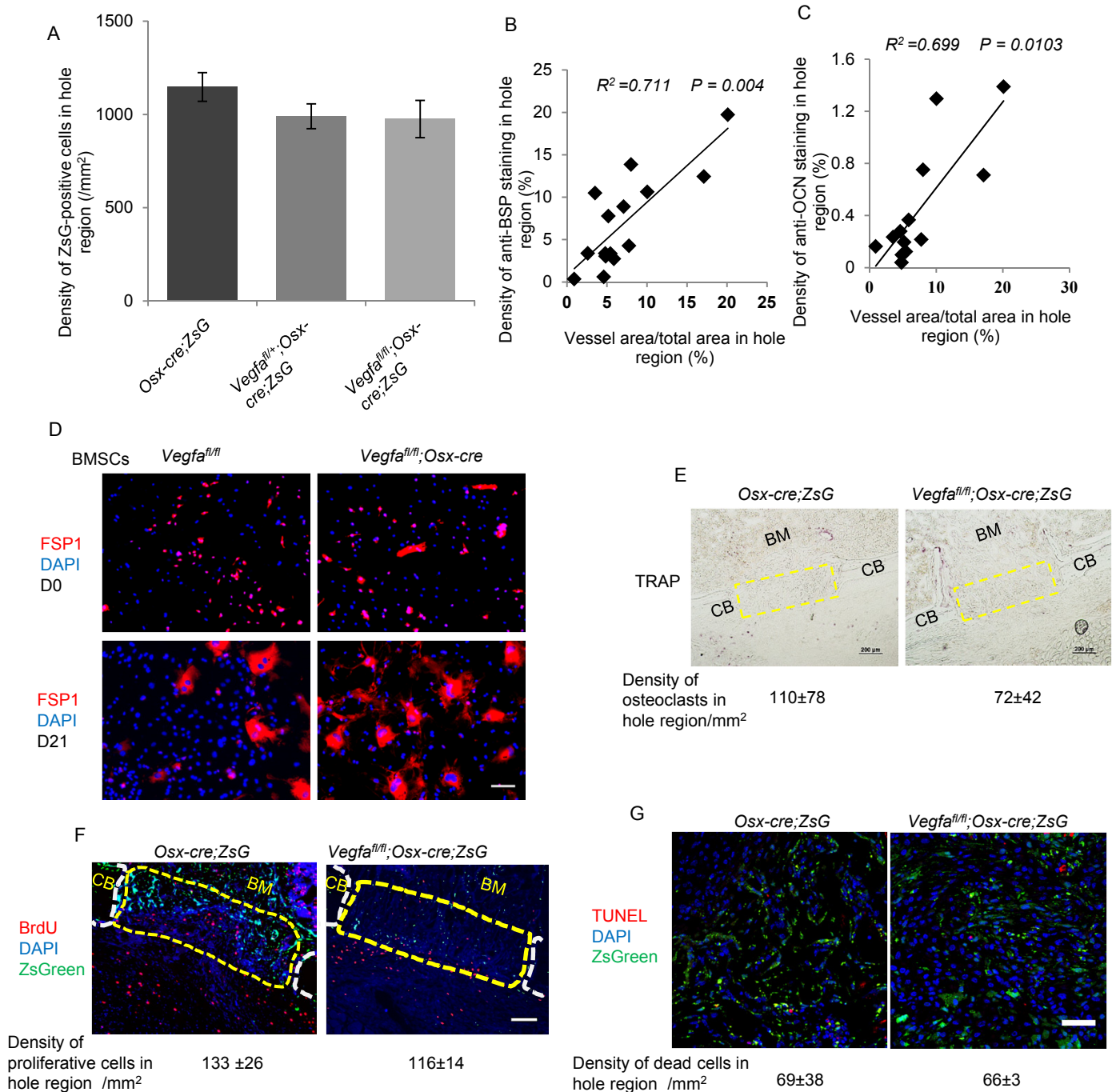


Figure S5. **Reduced angiogenesis and osteoblast differentiation in *Vegfa^{fl/fl};*Osx-cre;ZsG mice at PSD7.**

(A) Similar density of ZsG-positive cells in defect hole region in different genotypes, N=5-6. (B, C) Strong correlation between percentage of blood vessel areas and density of BSP (B) or OCN (C) stained areas in defect hole region. (D) Increased numbers of FSP+ fibroblasts in BMSCs from *Vegfa^{fl/fl};*Osx-cre mice after 21 days of culture in mineralization medium with 100nM dexamethasone. Representative images from three independent experiments. (E) No significant difference in density of TRAP-positive osteoclasts in hole region of *Osx-cre;ZsG* and *Vegfa^{fl/fl};*Osx-cre;ZsG mice, N=3-4. (F, G) Similar density of BrdU labeled cells (F) and TUNEL-positive cells (G) in hole region of *Osx-cre;ZsG* and *Vegfa^{fl/fl};*Osx-cre;ZsG mice, N=5-6. Yellow stippled rectangles: hole region. CB: cortical bone. Scale bars: 50µm (G), 100µm (D, F), 200µm (E). ANOVA with Tukey's post-hoc test (A), spearman's correlation coefficient test (B, C) and unpaired 2-tailed Student's *t*-test (E-G) were used.

Figure S6

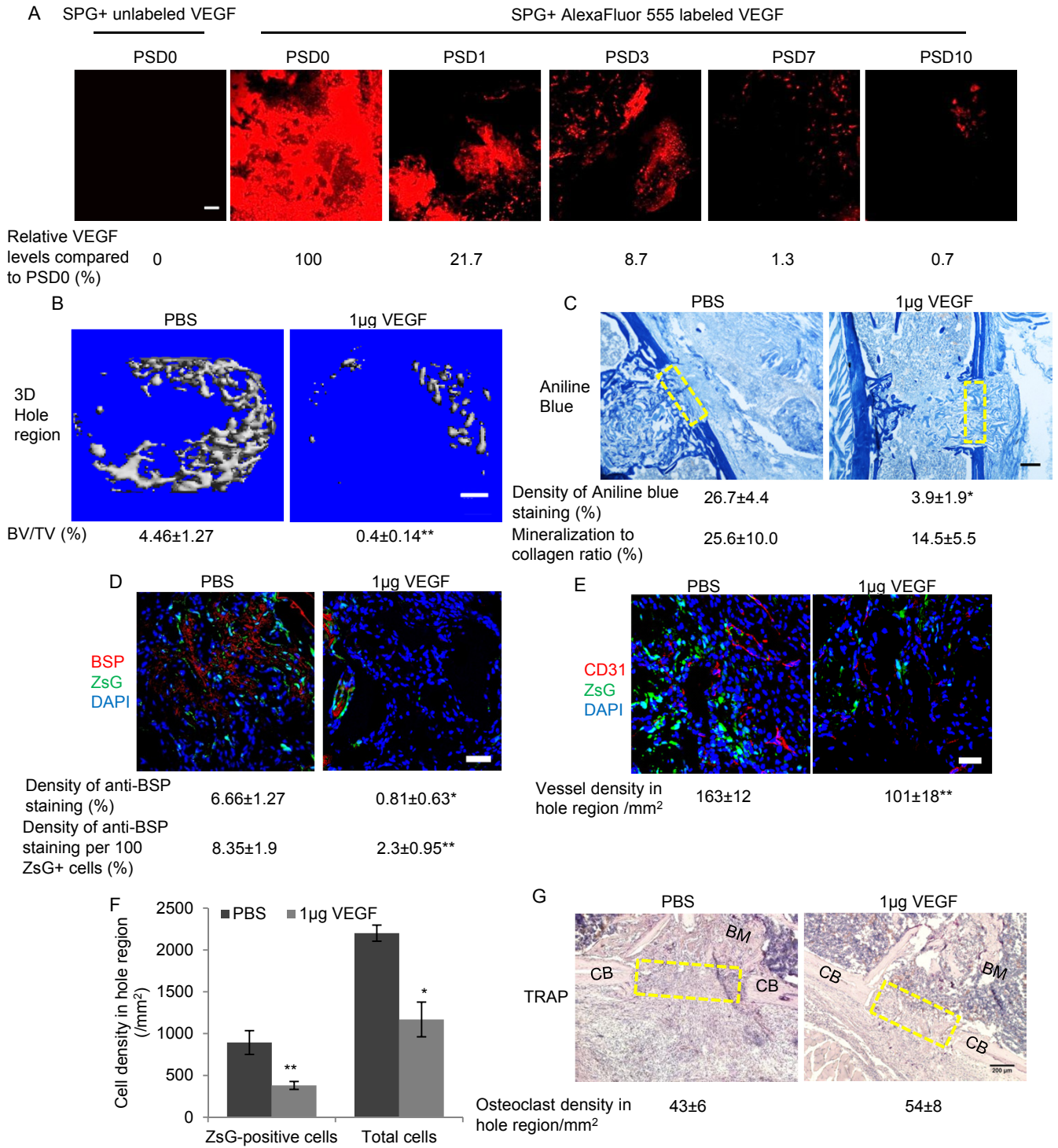


Figure S6. Treatment with 1µg VEGF in collagen sponges inhibits mineralized bone formation in cortical defects of *Osx-cre;ZsG* mice at PSD7. (A) Confocal image of the hole region containing absorbable collagen sponge (SPG) with AlexaFluor 555-labelled VEGF at various time points after surgery. The relative amount of VEGF remaining in SPG, based on fluorescence density, was calculated. Data represent two independent experiments. (B) Based on µCT, less mineralized bone formed in hole region in *Osx-cre;ZsG* mice treated with 1µg VEGF (BV/TV 0.4 ± 0.14 %) compared with PBS (4.46 ± 1.27 %). (C) 1µg VEGF reduces density of aniline blue staining in hole region of *Osx-cre;ZsG* mice compared with PBS, but does not alter mineralization to collagen ratio. (D) 1µg VEGF reduces density of anti-BSP staining with or without normalization to total number of ZsG-positive cells in hole region of *Osx-cre;ZsG* mice. (E) Low density (101 ± 18 /mm²) of blood vessels (determined by anti-CD31 staining) in hole region of *Osx-cre;ZsG* mice treated with 1µg VEGF compared with PBS treatment (163 ± 12 /mm²). (F) Reduced density of ZsG-positive cells and total cells in hole region of *Osx-cre;ZsG* mice treated with VEGF compared with PBS treatment. (G) No difference in low density of TRAP-positive osteoclasts in hole region of mice treated with VEGF or PBS. Yellow stippled rectangles: hole regions (C, G). CB: cortical bone. Scale bars: 100 µm (A, B), 200µm (C, G), 50 µm (D, E), N=4-5 (B-G). Unpaired 2-tailed Student's *t*-test was used. *, $P < 0.01$; **, $P < 0.05$.

Figure S7

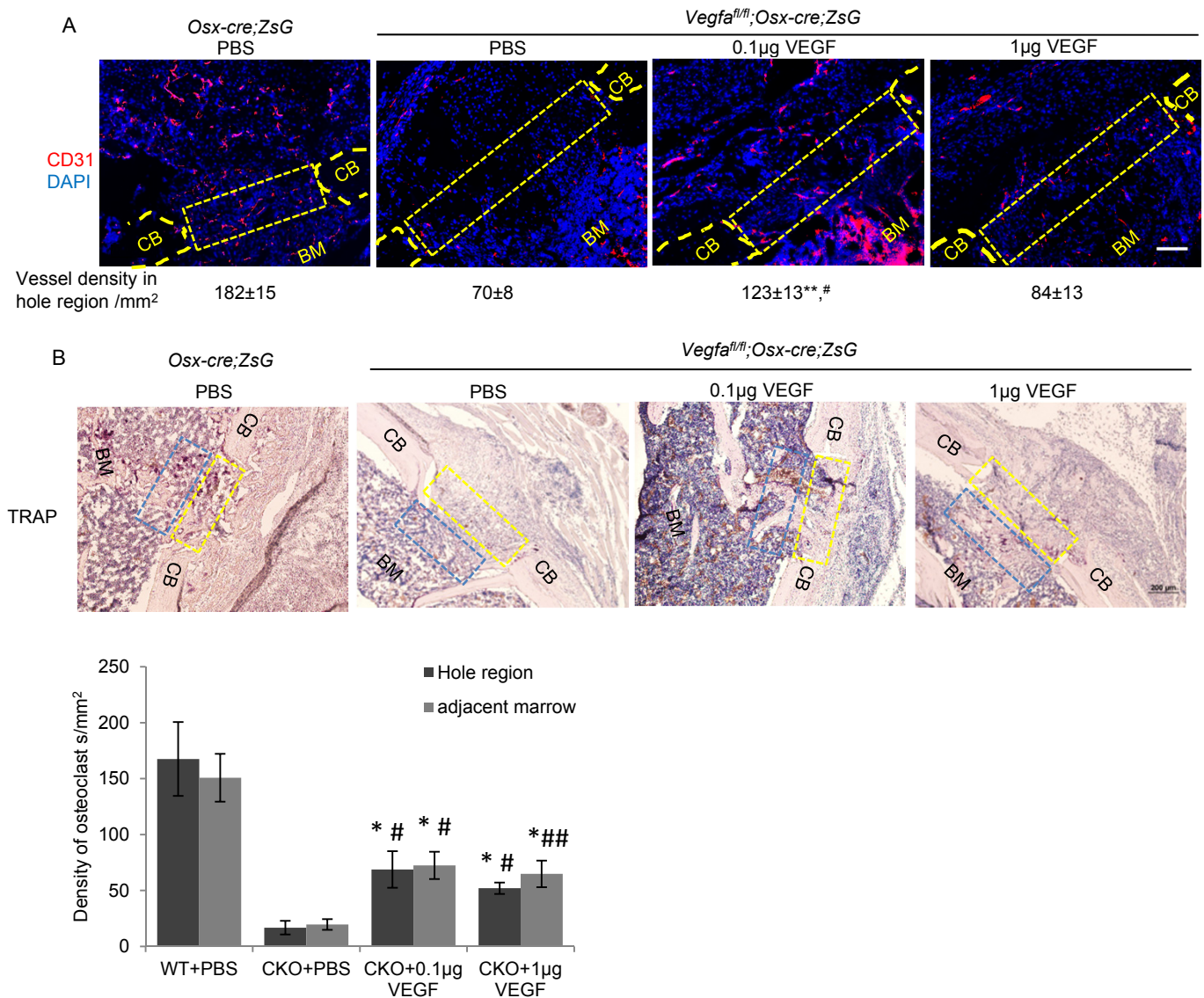


Figure S7. Blood vessel formation and osteoclast recruitment in cortical defects with delivery of PBS or recombinant VEGF at PSD10. (A) Enhanced density ($123 \pm 13/\text{mm}^2$) of blood vessels (based on anti-CD31 staining) in defect hole region of *Vegfa^{fl/fl};Osx-cre;ZsG* mice treated with 0.1µg VEGF compared with PBS ($70 \pm 8/\text{mm}^2$) or 1µg VEGF ($84 \pm 13/\text{mm}^2$). N=5-6 mice for each treatment group. (B) Density of TRAP-positive osteoclasts in hole region and adjacent area of injured BM. Scale bars: 100µm (A), 200µm (B), N=5-6. Yellow stippled rectangles: hole region (A, B); blue stippled rectangles: adjacent bone marrow regions (B). CB: cortical bone. WT: *Osx-cre;ZsG* mice. CKO: *Vegfa^{fl/fl};Osx-cre* mice. Unpaired 2-tailed Student's *t*-test was used. *, #, $P < 0.01$; **, ##, $P < 0.05$. * vs. *Osx-cre;ZsG*+PBS. # vs. *Vegfa^{fl/fl};Osx-cre;ZsG*+PBS.

Figure S8

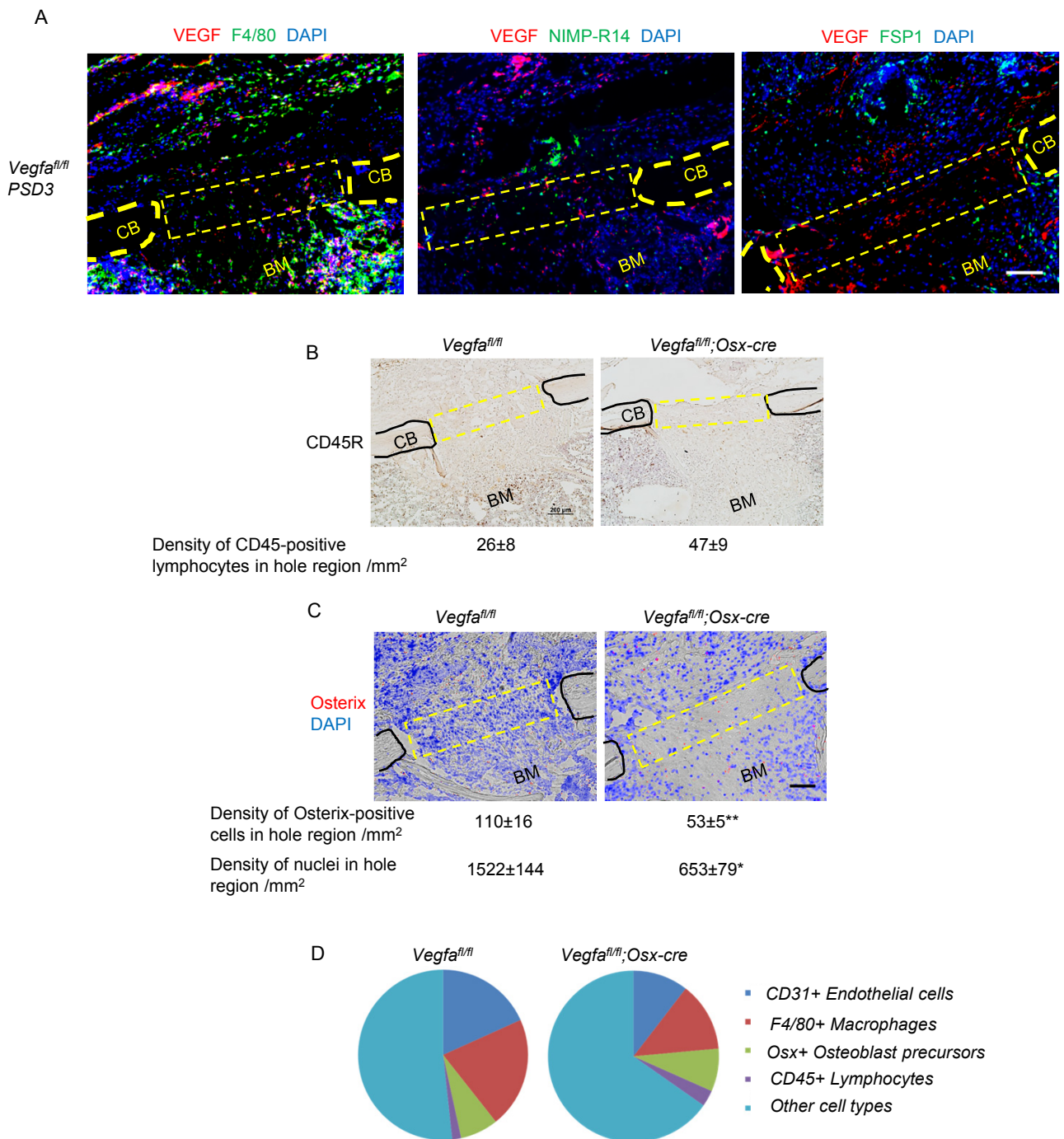
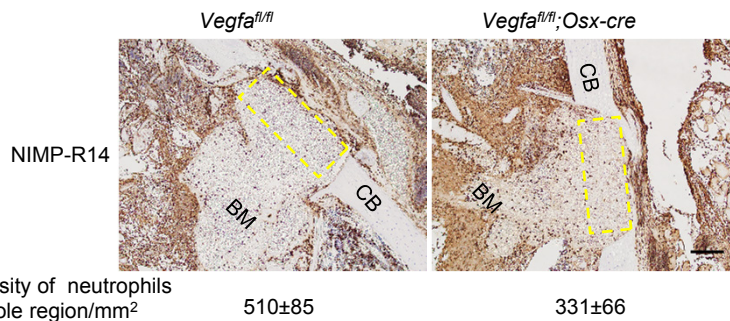


Figure S8. VEGF promotes cell infiltration at PSD3. (A) Co-staining with antibodies against VEGF, macrophage marker F4/80, neutrophil marker NIMP-R14 or fibroblast marker FSP1 in injury sites of *Vegfa*^{fl/fl} mice at PSD3. Representative images from three independent experiments. (B) Similar density of CD45R-positive lymphocytes in hole region of *Vegfa*^{fl/fl}; *Osx-cre* and *Vegfa*^{fl/fl} mice, N=4-6. (C) Low density of osterix-positive osteoblast precursor cells ($53 \pm 5 / \text{mm}^2$) and total cells ($653 \pm 79 / \text{mm}^2$), the latter determined by counting total numbers of nuclei, in hole region of *Vegfa*^{fl/fl}; *Osx-cre* compared with *Vegfa*^{fl/fl} mice ($110 \pm 16 / \text{mm}^2$ and $1522 \pm 21 / \text{mm}^2$), N=5-6. (D) Percentage of different cell types in hole region of *Vegfa*^{fl/fl}; *Osx-cre* and *Vegfa*^{fl/fl} mice. Yellow stippled rectangles: hole region. CB: cortical bone. Scale bars: 100 μm (A, C), 200 μm (B). Unpaired 2-tailed Student's *t*-test was used. *, $P < 0.01$; **, $P < 0.05$.

Figure S9

A	PSD0		PSD1		Normal range
	<i>Vegfa^{fl/fl}</i>	<i>Vegfa</i> CKO	<i>Vegfa^{fl/fl}</i>	<i>Vegfa</i> CKO	
WBC (K/ μ L)	3.6 \pm 0.3	3.5 \pm 0.8	3.5 \pm 0.4	4.3 \pm 0.4	1.8-10.7
NE (K/ μ L)	0.4 \pm 0.1	0.6 \pm 0.1	1.2 \pm 0.1*	0.9 \pm 0.1*	0.1-2.4
LY (K/ μ L)	3.1 \pm 0.3	2.9 \pm 0.7	2.2 \pm 0.3	3.3 \pm 0.3	0.9-9.3
NE %	11.1 \pm 1.6	17.8 \pm 2.7	34.5 \pm 3.1*	20.3 \pm 1.2	6.6-38.9
LY %	85.4 \pm 2.1	79.1 \pm 2.8	61.1 \pm 3.5*	76.7 \pm 1.6	55.8-91.6
RBC (M/ μ L)	8.9 \pm 0.4	8.7 \pm 0.7	9.0 \pm 0.4	8.8 \pm 0.4	6.4-9.4
Hb (g/dL)	10.9 \pm 0.4	11.1 \pm 0.9	11.5 \pm 0.4	10.8 \pm 0.4	11.0-15.1
HCT %	44.9 \pm 2.4	43.4 \pm 3.0	44.6 \pm 2.2	43.7 \pm 2.5	35.1-45.4
PLT (K/ μ L)	589.3 \pm 45	417.3 \pm 76.5	581.5 \pm 36.6	578.9 \pm 22.1	592-2972

B



C

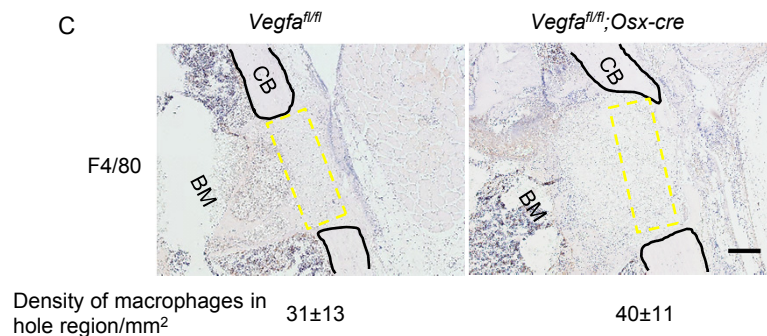


Figure S9. **Alteration of peripheral blood cells and local infiltration of inflammatory cells during acute inflammation.** (A) Complete analysis of peripheral blood from mice before and 24 hours after surgery, N=6-7. (B, C) Similar density of NIMP-R14 positive neutrophils (B) and F4/80-positive macrophages (C) in defect hole region of *Vegfa^{fl/fl};Osx-cre* and *Vegfa^{fl/fl}* mice at PSD1, N=4-7. Scale bar: 200 μ m (B, C). Yellow stippled rectangles: hole region. CB: cortical bone. Unpaired 2-tailed Student's *t*-test was used. *, $P < 0.01$. *, PSD1 vs. PSD0.

Figure S10

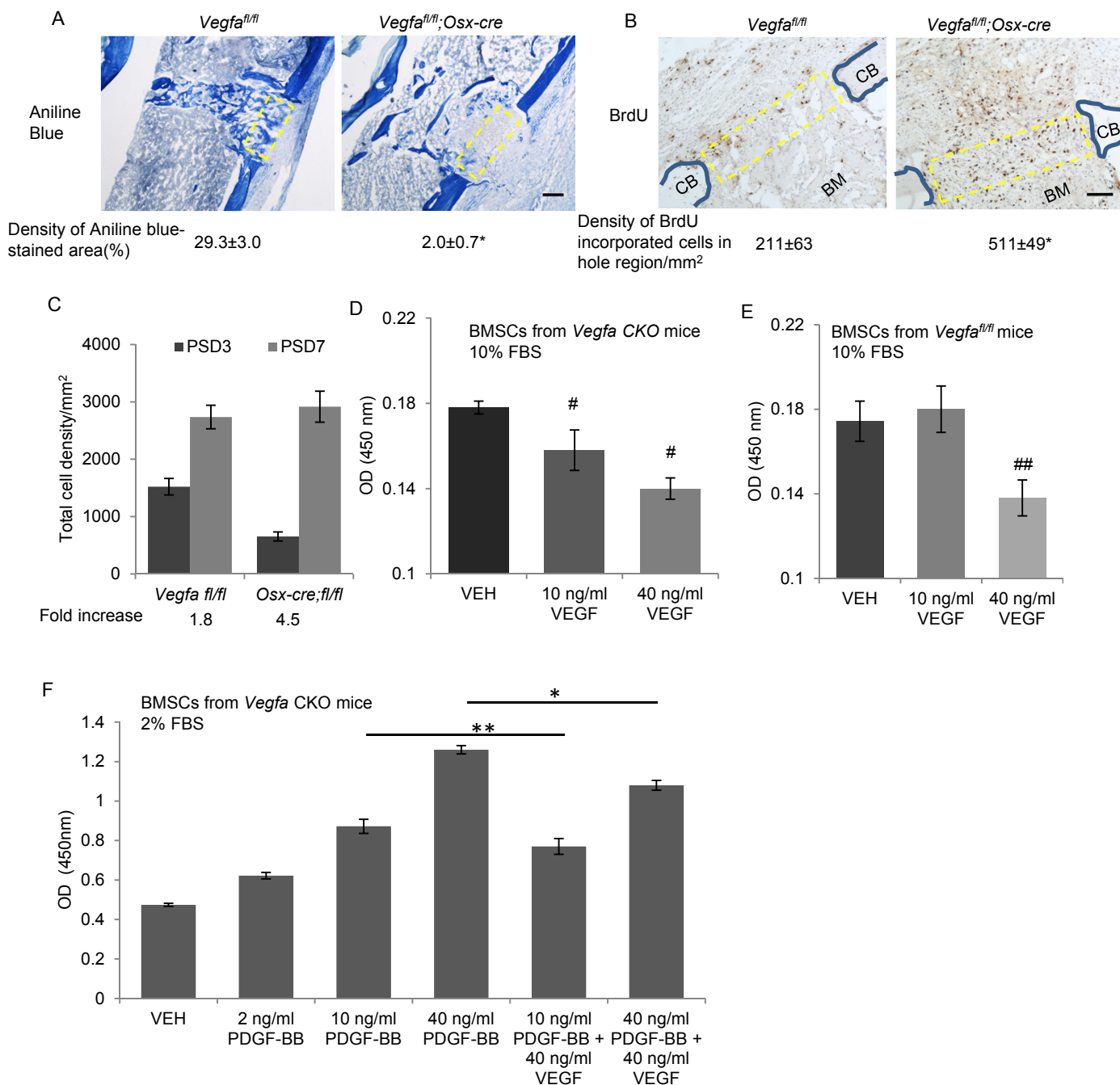


Figure S10. **Increased cell proliferation and decreased collagen accumulation in *Vegfa^{fl/fl};Osx-cre* mice at PSD5.** (A) Reduced density ($2.0 \pm 0.7\%$) of aniline blue-stained areas in hole region of *Vegfa^{fl/fl};Osx-cre* mice compared with *Vegfa^{fl/fl}* mice ($29.3 \pm 3.0\%$), N=4-5. Scale bar: 200 μ m. (B) Increased density ($511 \pm 49/\text{mm}^2$) of BrdU incorporated cells in hole region of *Vegfa^{fl/fl};Osx-cre* mice compared with *Vegfa^{fl/fl}* mice ($211 \pm 63/\text{mm}^2$), N=3-4. Scale bar: 100 μ m. (C) Fold increase in total cell density in hole region of *Vegfa^{fl/fl};Osx-cre* and *Vegfa^{fl/fl}* mice from PSD3 to PSD7. (D-F) Proliferation of BMSCs cultured in medium for 48 hour monitored by CCK8. OD_{450nm} represents relative cell number. At least 4 wells used for each group; data are representative of three independent experiments. Yellow stippled rectangles: hole region. CB: cortical bone. Unpaired 2-tailed Student's *t*-test was used. *, #, $P < 0.01$; **, ##, $P < 0.05$. # vs. VEH (D, E)

Figure S11

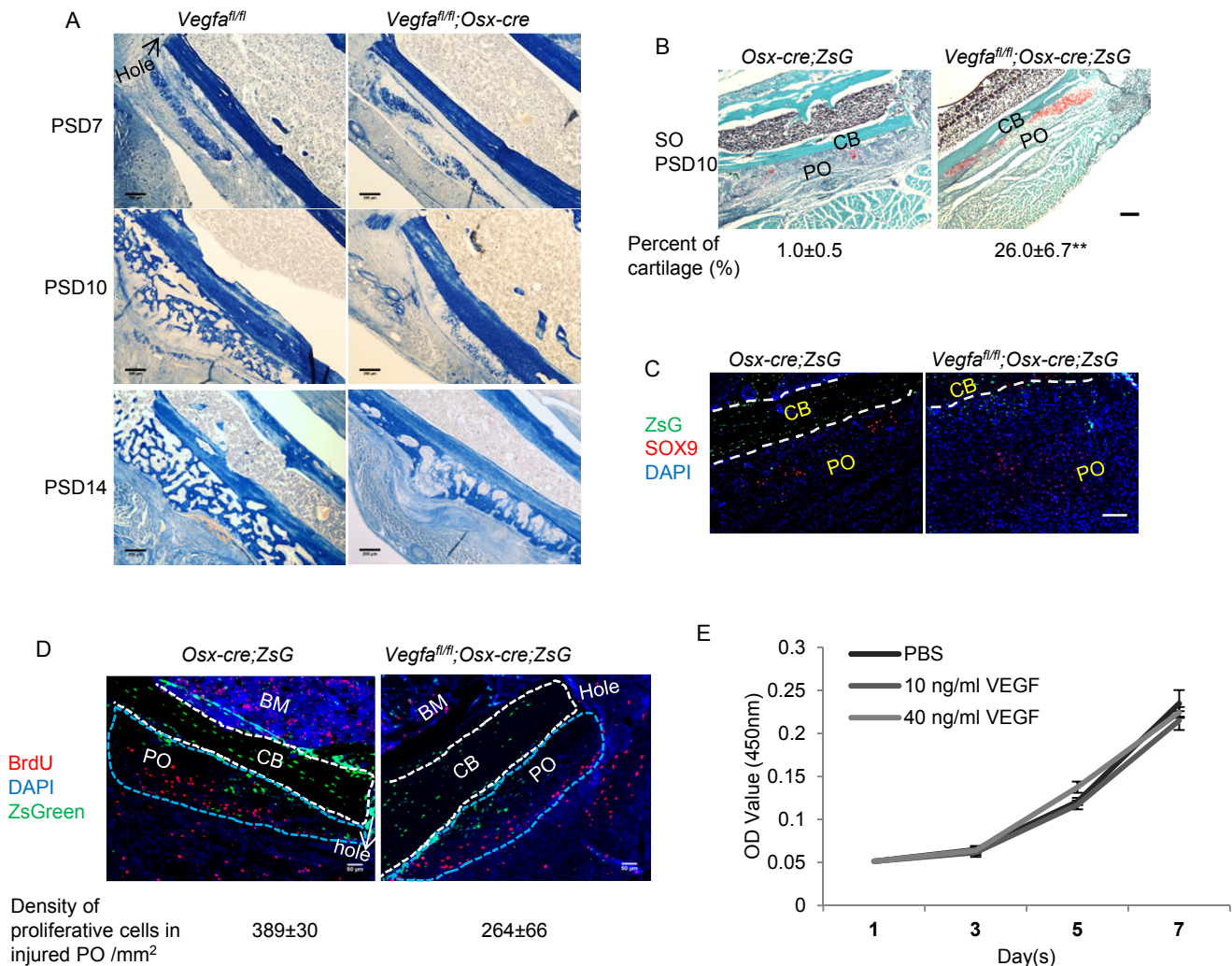


Figure S11. **Delayed replacement of cartilaginous callus by bony callus in *Vegfa^{fl/fl}; Osx-cre* mice.** (A) Aniline blue staining on sections from mice at PSD7, PSD10 and PSD14 shows bony callus in periosteum. Representative images from 4-8 mice for each genotype. (B) Increased percentage ($26.0 \pm 6.7\%$) of safranin O (SO)-stained cartilage in injured periosteum of *Vegfa^{fl/fl}; Osx-cre; ZsG* mice compared with *Osx-cre; ZsG* mice ($1.0 \pm 0.5\%$), $N=3-5$. (C) Increased number of SOX9-positive chondrocytes in injured periosteum of *Vegfa^{fl/fl}; Osx-cre; ZsG* mice compared with *Osx-cre; ZsG* mice; few ZsG-positive osteoblast lineage cells express SOX9. Representative images from 3-4 mice for each genotype. (D) Similar density of BrdU labeled cells in injured PO of *Osx-cre; ZsG* and *Vegfa^{fl/fl}; Osx-cre; ZsG* mice, $N=4-5$. (E) Administration of recombinant VEGF does not affect proliferation of primary murine chondrocytes; The data are representative of three independent experiments. CB: cortical bone (white stippled area); PO: periosteum (blue stippled area). Scale bars: 50 μ m (D), 100 μ m (C), 200 μ m (A, B). Unpaired 2-tailed Student's *t*-test was used. **, $P<0.05$.

Figure S12

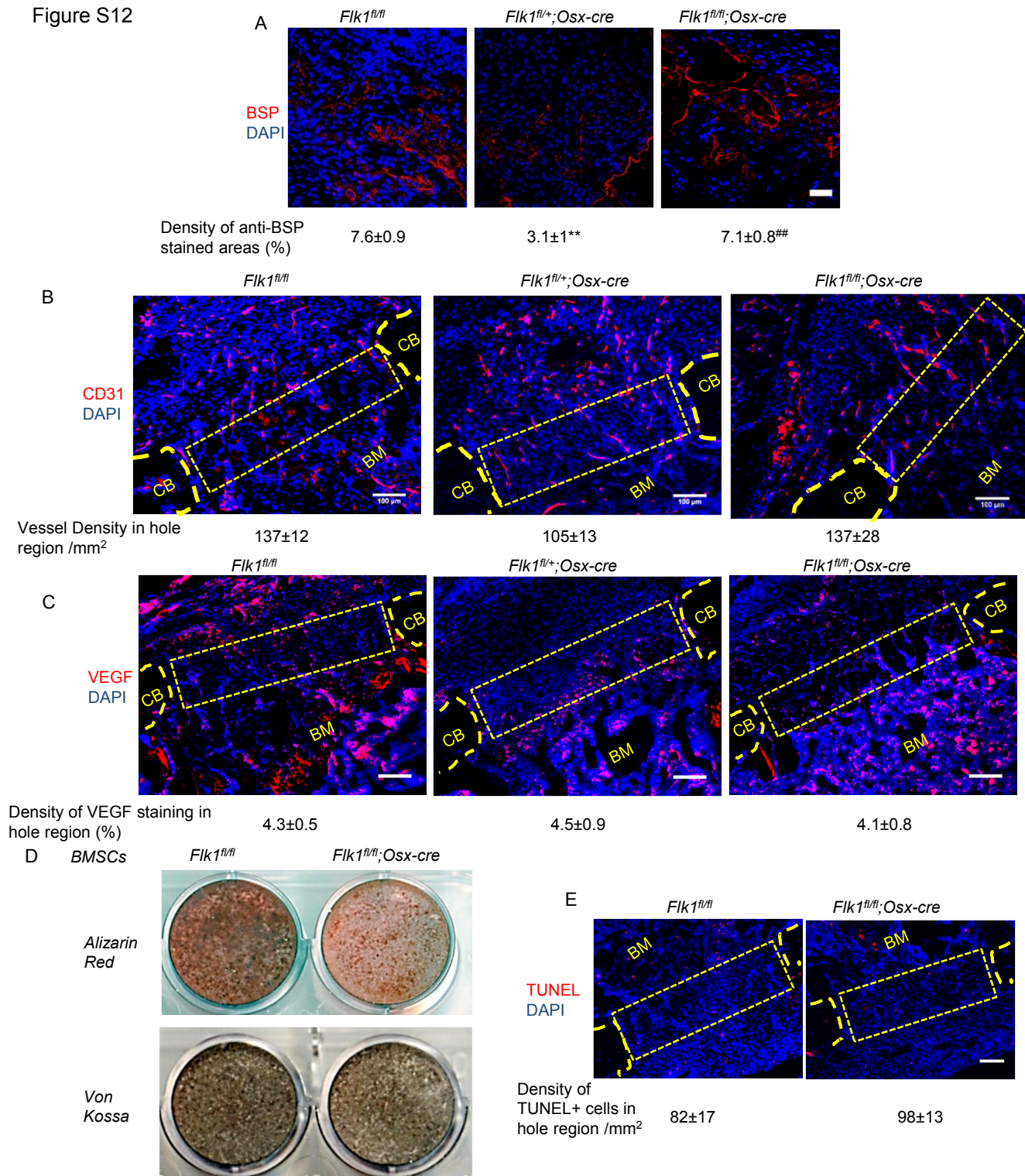


Figure S12. **Increased osteoblast maturation and mineralization in defects of *Flk1^{fl/fl};Osx-cre* mice at PSD7.** (A) Low density of anti-BSP stained areas in hole region of *Flk1^{fl/+};Osx-cre* mice compared with *Flk1^{fl/fl};Osx-cre* and *Flk1^{fl/fl}* mice at PSD7, N=4-7. (B, C) Similar density of blood vessels (based on CD31 staining) (B) and VEGF levels (C) in hole region of different genotypes, N=4-7. (D) Alizarin red and Von Kossa staining of BMSCs from *Flk1^{fl/fl}* or *Flk1^{fl/fl};Osx-cre* mice after 21 days of culture in mineralization medium with 100nM dexamethasone. Representative images from three independent experiments. (E) Similar density of TUNEL+ cells in hole region of *Flk1^{fl/fl}* and *Flk1^{fl/fl};Osx-cre* mice, N=7. Scale bars: 50µm (A), 100µm (B, C, E). Yellow stippled rectangles: hole region. CB: cortical bone. ANOVA with Tukey's post-hoc test (A-C) and unpaired 2-tailed Student's *t*-test (E) were used. **, ## *P*<0.05. ** vs. *Flk1^{fl/fl}*. ## vs *Flk1^{fl/+};Osx-cre*.

Figure S13

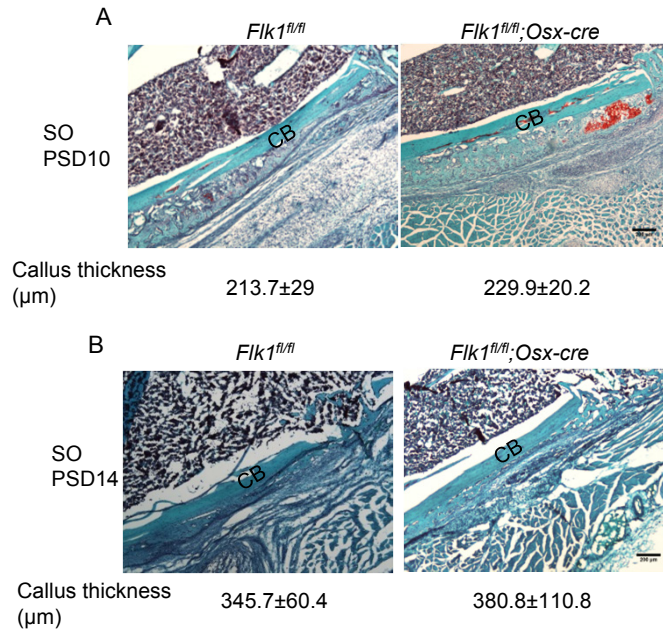


Figure S13. **Periosteal endochondral ossification is not altered when *Vegfr2* is removed from osteoblastic cells.** (A) Safranin O-stained cartilage in periosteum distal to hole region in *Flk1^{fl/fl}* and *Flk1^{fl/fl};Osx-cre* mice at PSD10. Similar percentage of stained cartilage and callus thickness, represented by average distance from edge of periosteal callus to cortical bone, in at least 3 tissue sections, N=3-5 for each genotype. (B) Almost no safranin O-stained cartilage in either *Flk1^{fl/fl}* and *Flk1^{fl/fl};Osx-cre* mice at PSD14. No difference in periosteal callus thickness, N=3-5. CB: cortical bone. Scale bar: 200 μm . Unpaired 2-tailed Student's *t*-test was used.

Figure S14

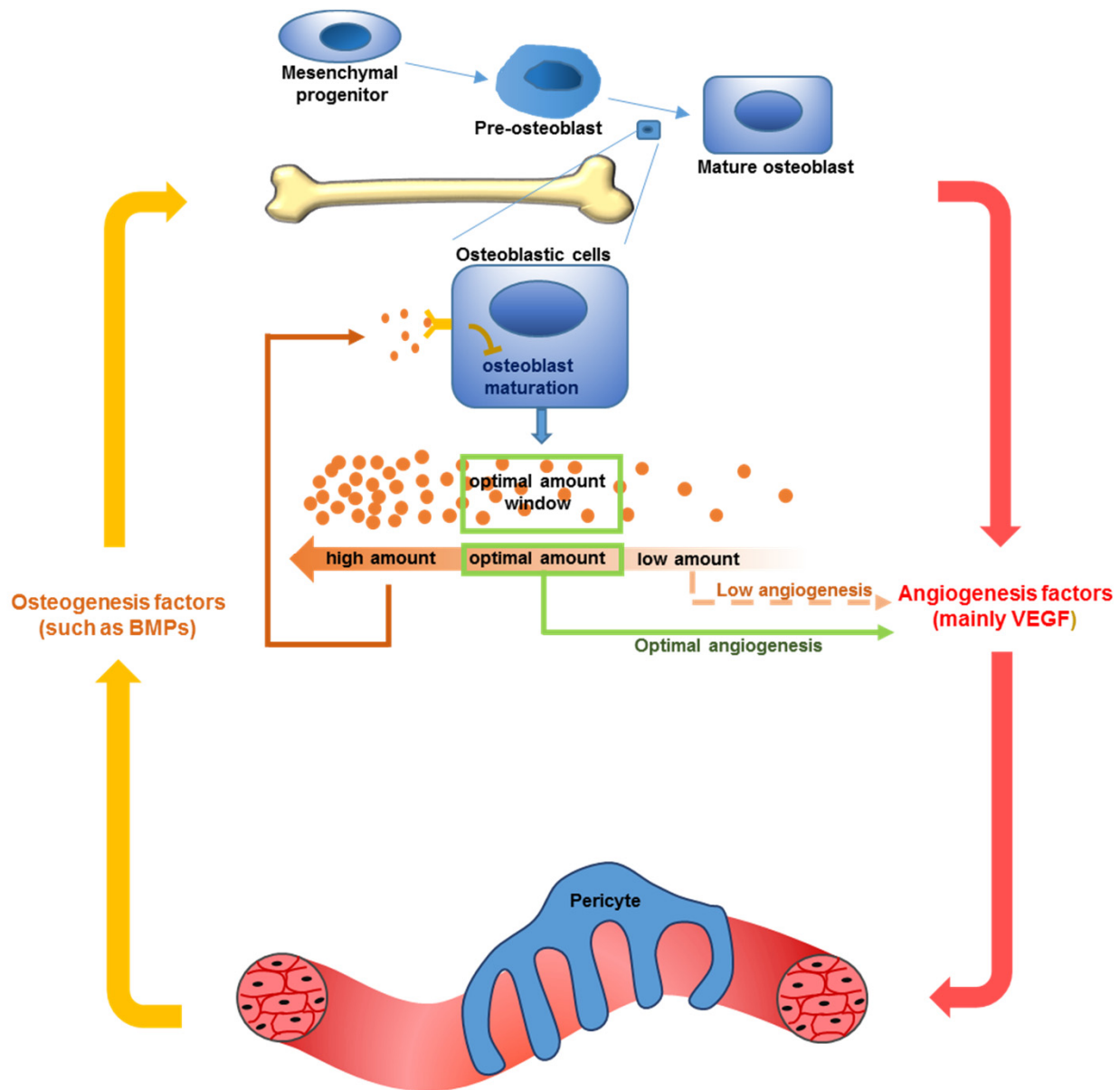


Figure S14. **Diagrams summarizing roles of osteoblast-derived VEGF in bone defect healing.** In response to hypoxia during inflammation, osteoblasts release angiogenic factors, including VEGF, which induce proliferation and migration of endothelial cells. Increased vasculogenesis and angiogenesis bring bone-forming progenitors as well as nutrition, oxygen and minerals. In addition, vascular cells release osteogenic factors, such as BMP2, further promoting osteoblast differentiation and mineralization. In the bone healing process, physiological levels of VEGF are important. Reduced VEGF levels in osteoblasts result in interrupted communication between bone and blood vessels, and compromised bone healing. Levels of VEGF beyond physiological levels have detrimental effects on bone repair, likely due to inhibition of osteoblastic maturation and mineralization via stimulated VEGFR2 signaling.